Enhancing permeability of a woven glass-fabric preform with 3D spacers

Damiano Salvatori[1], Baris Caglar[2], Véronique Michaud[3]

Laboratory for Processing of Advanced Composites (LPAC)
Institute of Materials (IMX), Ecole Polytechnique Fédérale de Lausanne (EPFL)
Station 12, 1015 Lausanne, Switzerland
Email: [1]damiano.salvatori@epfl.ch, [2]baris.caglar@epfl.ch, [3]veronique.michaud@epfl.ch
Web Page: https://lpac.epfl.ch/

Keywords: resin transfer molding, flow enhancement, permeability, dual-scale flow, 3D-printing

Abstract
Resin transfer molding (RTM) is a process for production of continuous fiber-reinforced polymer composites in which the liquid matrix is injected in a rigid mold containing the reinforcing fabric, which has to be fully impregnated prior to solidification. The impregnation time is inversely proportional to fabric permeability, representing the major limit of this technique for high viscosity fluids. The goal of the present study is to reduce the impregnation time in RTM process by introducing a second solid phase in the fabric stack. Specifically, the investigation focused on the use of three-dimensional structures fabricated in poly(lactic acid) (PLA) by 3D-printing as flow-enhancers. A square-lattice geometry was chosen for the 3D-spacers, and the influence of mesh-size on compaction and permeability of sandwich-like preforms investigated. An increase of almost two orders of magnitude in permeability was observed, which, however, resulted in exacerbated dual scale flow behavior. Alternative impregnation strategies were assessed in order to find an optimum between impregnation time and quality. As a proof of concept, a composite plate was produced via RTM with an epoxy resin and a PLA spacer and its meso-structure observed with an optical magnifier.

1. Introduction

Permeability is a measure of how easily a porous medium is impregnated by a fluid [1]. In RTM manufacturing process, the kinetics of impregnation of a reinforcing fabric, compacted and confined inside a mold, by the liquid resin linearly depends on permeability, which is a function of the fiber volume fraction, fiber radius, and fiber geometrical arrangement [2]. Textiles are characterized by a bimodal distribution of pore sizes, with micro-pores in the space within the fiber bundles (intra-tow space) and meso-pores between them (inter-tow space). Previous research showed that enhancing the dual-scale nature of fabrics is the key to permeability enhancement [3-5], but at the price of possible deterioration of mechanical properties of the final composite [6]. In addition, it results in non-uniform fluid flow with consequent risk of void formation [7], which also detrimentally affects the quality of the final part.

Meso-channels formed upon compaction of a non-crimp fabric preform and oriented along the flow direction were shown to lead to a significant increase of permeability [8]. In addition, if the size of channels is much larger than the distance between single fibers inside a bundle, permeability of the whole stack can be simply predicted by the size and shape of the channels, since intra-tow flow becomes negligible. However, the channel's geometry is not known a priori, and depends on the number of layers and degree of compaction, as well as on the care taken during cutting and lay-up. Indeed, nesting between adjacent layers was observed to partially obstruct the channels and modify their shape. In addition, exaggerated dual-scale flow resulted in large unsaturation of the fabric preform.

In the present study, an additional solid-phase is introduced in the preform to modify its architecture so as to induce formation of flow-enhancing channels. The concept is schematically shown in Fig. 1a. The spacer is placed in the core of a sandwich-like preform. Predictably, the fluid will flow preferentially along the plane in the core region, from inlet to outlet, and later through the thickness to impregnate the

fabric, similarly to flow-enhancement in vacuum-infusion, where a bi-dimensional grid is placed between the fabric stack and the flexible vacuum-bag. However, in the present case the spacer is three-dimensional, placed in the middle of the fabric stack, and meant to remain embedded in the final part. Three-dimensional spacers featuring channels along the flow direction were fabricated by 3D-printing. The influence of channels width on compaction and permeability was experimentally investigated on PLA spacers and a woven glass-fabric. Strategies to optimize the impregnation time, and reduce the risk of void entrapment, were investigated. Finally, a real part was produced via RTM as a proof of concept.

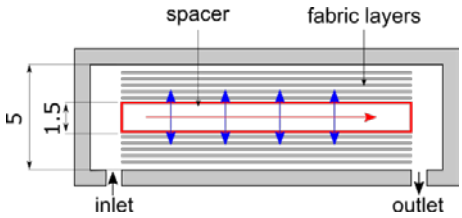

Figure 1. (a) Schematic side-view of a sandwich-like preform, showing in-plane (red arrow) and transverse (blue arrows) flow (dimensions in mm).

2. Materials and methods

2.1 Materials

3D spacers were fabricated in PLA (TreeD Filaments). As reinforcing fabric, a twill 2×2 glass-fabric (G-WEAVE®, Chomarat), with areal weight of 600 g/m^2, was used [8]. An aqueous solution of poly(ethylene glycol) (PEG) (M_w = 35 kDa, Sigma Aldrich) at a concentration of 16.7% by weight (viscosity 0.111 Pa·s at 20°C, density 1.026 g/ml) was used as test fluid for flow experiments; a small amount of food colorant was added for contrast enhancement [8]. For plate production via RTM, an epoxy resin Araldite®LY8615 with hardener Aradur®8615, at a mixing ratio of 2:1, was used as matrix; according to the manufacturer, the gel time of this mixture is between 34-38 min at 80°C and 16-20 min at 100°C, and initial viscosity in the range 80-160 mPa·s at 40°C.

2.2 Design and fabrication of 3D spacers

2.2.1 Spacers design

The spacer design was performed on 3D modeling software SketchUP. It was conceived as a three-dimensional square lattice, where the repeating unit is a three-dimensional frame with solid walls along the flow direction (Fig. 2a). The final structure is an array of solid beams and channels along the flow direction, kept together by thinner transverse beams (Fig. 2b). The longitudinal beams are the structural components of the spacer, and they are accountable for bearing the compaction of the fabric. Beams' thickness t and width b were kept constant for all the structures to 1.5 and 1 mm, respectively. The spacers feature rectangular channels along the flow direction of constant height h = 1 mm and width w. Square gaps of size $w \times w$ allow through-thickness flow. Channel width w was varied from 2 to 6 mm; increase of spacer permeability, both in-plane and out-of-plane, and concurrent decrease of compressive stiffness, are expected for larger w. A too small mesh size could result in an excessively stiff structure, which would require too high pressure for compaction. On the other hand, a too large mesh size could cause the fabric to nest in the transverse gaps and eventually block the channels. Another meaningful parameter is b, which would affect the stiffness of the longitudinal beams, but which was kept constant.

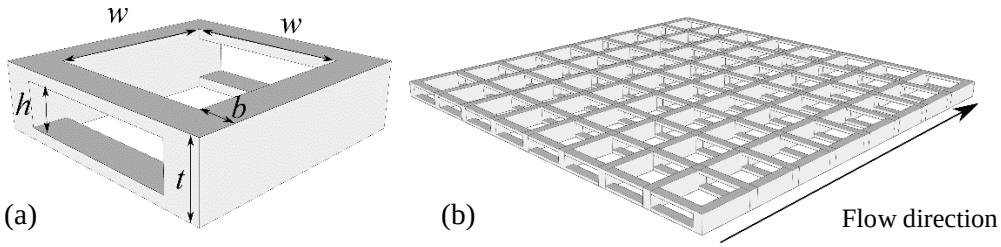

Figure 2. 3D model design of a unit cell (a) and of a whole spacer (b); t = 1.5 mm, b = 1 mm, h = 1 mm, w variable.

2.2.2 Fabrication by 3D-printing

Spacers were fabricated in PLA using a Fused Deposition Modeling (FDM) technique, on a 3D-Printer Ultimaker 2+. PLA was extruded through a nozzle of 0.25 mm diameter at a temperature of 210°C, and deposited on a heated bed at 60°C; nozzle speed was set at around 25 mm/s. Five different mesh sizes were investigated, with gap width w varying from 2 mm to 6 mm (Fig. 3a). Square spacers of side ~ 3 cm were used for compression and compaction tests (Fig. 3a). Additional spacers of size 5 cm × 20 cm (Fig. 3b) were printed for flow studies and production of a composite plate via RTM.

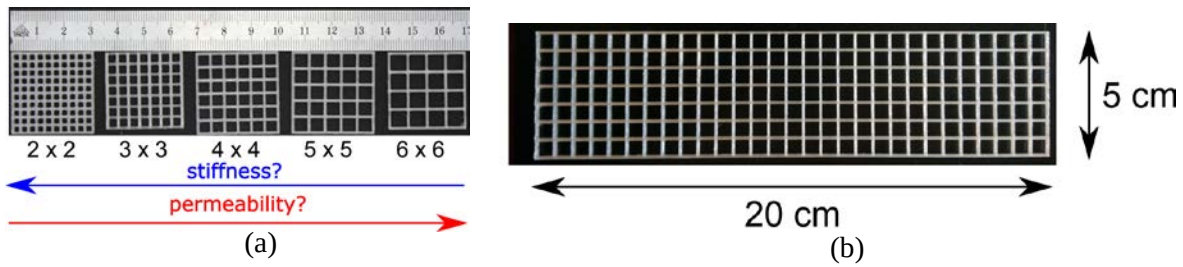

Figure 3. (a) Spacers used for compaction and compression tests and (b) for flow studies and plate production via RTM (mesh size 6 × 6 is shown).

2.3. Experiments

2.3.1 Preform structure

A sandwich-like preform architecture was investigated both for compaction and permeability experiments (Fig. 4). Ten layers of G-WEAVE were laid with a spacer in the middle (between layers 5 and 6) and with the fiber bundles parallel to the spacer's beams. The sandwich was compacted to 5 mm thickness cavity, which makes a global fiber volume fraction of 45.8%. However, the fabric is confined to a thickness of 3.5 mm, which gives a local fiber volume fraction of 65.4%.

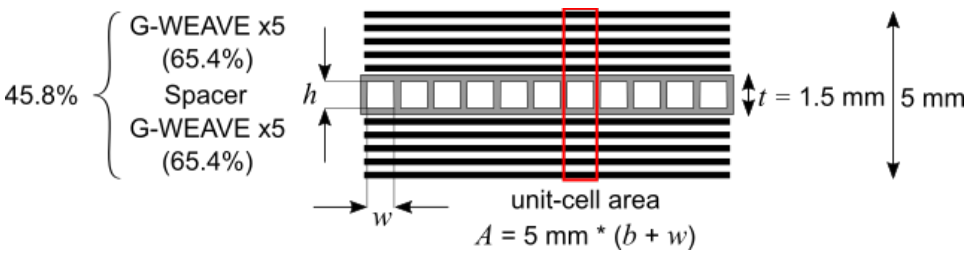

Figure 4. Schematic representation of the front-view of a sandwich-like preform (h, w, t and b are defined in Fig. 2a and A is the area of a cross-sectional unit-cell of the sandwich stack).

2.3.2 Compaction

Measurements of compaction pressure vs. thickness of sandwich-like preforms (Fig. 4) were performed on an ultimate testing machine *Walter + Bai AG Series LFL 125kN*, using a 10 kN load cell for force measurement. Samples were placed between two metal plates, and the upper plate was displaced at a constant speed of 1 mm/min. For each mesh size, three different samples of size around 3 cm × 3 cm (Fig. 3a) were printed and tested. Ten freshly-cut layers of G-WEAVE of size 5 cm × 5 cm, hence larger than the spacers, were hand-cut and laid all with the same orientation. Three tests on plain fabric (without spacer) were also performed. The compaction pressure was calculated by dividing the measured force by the area of the spacer (≈ 9 cm^2), which was carrying the load. The stack was compacted down to a thickness of 5 mm. Force was continuously measured at this constant thickness for around 4 min, so as to evaluate the fabric relaxation.

2.3.3 Flow experiments

Flow experiments were conducted using the setup shown in Fig. 5, consisting in an RTM mold with a flat rectangular cavity and a transparent top allowing flow visualization; a pressure-pot for constant-pressure injection; and a scale for measurement of the mass of the out-coming fluid. The sandwich preforms were compacted in the mold cavity of thickness 5 mm. For these tests, PLA-spacers of size 5 cm × 20 cm were used (Fig. 3b), and the glass-fabric was cut to the same size. Two sets of experiments were carried out. In the first one, the saturated permeability of sandwich preforms with spacers of varying mesh-size was measured and compared against that of the plain fabric. From the first series of tests, it was found that it is not straightforward to achieve full saturation, because the fluid flows too fast at the outlet, leaving the fabric largely unsaturated. Therefore, in the second series of tests one type of architecture (6 × 6) was selected in order to investigate different impregnation strategies.

In saturated permeability measurements, the mold was filled with the test fluid, and the flow rate Q_{out} at the outlet measured to obtain the saturated permeability K_{sat} from Darcy's law for unidirectional, constant-pressure, in-plane flow:

$$K_{sat} = \frac{Q_{out}\eta L}{A_s\,\Delta P} \tag{1}$$

where η is the fluid viscosity, L the preform length, A_s the sandwich cross-sectional area (50 mm × 5 mm) and ΔP the pressure difference between inlet and outlet. Data of fluid pressure and temperature at the inlet and mass at the outlet were recorded with a computer.

In the second series, the fluid was injected with the same applied pressure (≈ 0.6 bar), and vacuum was pulled in the mold cavity from the outlet for 1 min prior to the injection and during the injection. In the first two experiments the fluid was slowed down so as to prevent it to flow out of the mold and force transverse fabric impregnation. The "brake" mechanism was different: in the first experiment, a dam-zone was created at the end of the fabric, making use of a microporous membrane which allows air but not a liquid to pass through (Goretex membrane); in the second one, once the fluid had reached the outlet, this latter was closed (i.e. no more vacuum was being pulled) while the inlet was kept open and more pressurized fluid was being injected. A third experiment without any spacer (i.e. 10 layers of G-WEAVE) was also conducted. All the experiments continued for at least 10 min in order to reach a full saturation state. Fluid infiltration was recorded with a digital camera Canon EOS 700D with a frame acquisition rate of 29 fps. The goal of these experiments was to compare filling times by image analysis. The video frames were subdivided in unit cells. A MatLab code was used to generate horizontal and vertical lines, which would follow the fiber bundles' borders. The images were binarised and saturation was defined for each cell at any frame using the fully saturated state (the final frame of the video) as a reference.

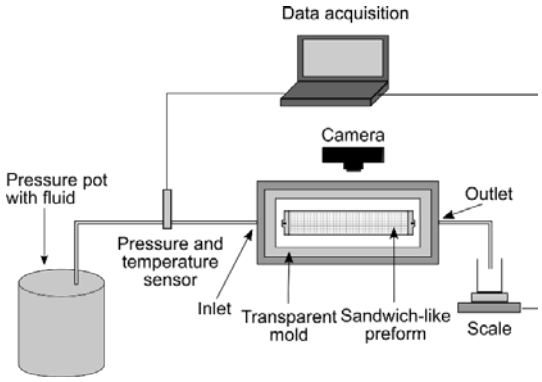

Figure 5. Setup for flow experiments.

2.3.4 Production of a plate

The "closed-outlet" strategy investigated with a model fluid was subsequently applied to the production of a composite plate via RTM and with a PLA-spacer of mesh-size 6 × 6 (Fig. 3b) and an epoxy resin as matrix. The plate was produced in the same setup used for flow experiments, which was also equipped with six heating cartridges embedded in the bottom steel part of the mold. The PLA-spacer and G-WEAVE layers were placed in the mold cavity in the same stacking sequence shown in Fig. 4, and the preform size was 5 cm × 20 cm. The resin was kept at room temperature (20°C) and injected at 1 bar of pressure in the mold pre-heated at 40°C. Vacuum was also applied at the outlet during the impregnation, and once the resin had reached the outlet, this was closed and through-thickness impregnation of the fabric was forced by injecting more fluid at the inlet. After the impregnation was visibly achieved, mold temperature was raised to the curing temperature of 80 °C. The resin was let to cure in the mold for 3 h under pressure. The meso-structure of the final plate's cross-section was observed with an optical magnifier.

3. Results and discussion

3.1 Compaction

Fig. 6a shows the pressure evolution during compaction and relaxation at constant thickness (5 mm). Unsurprisingly, the pressure required for compaction is higher for smaller mesh-size, whose stiffness is higher due to the larger number of beams carrying the load. However, normalization of relaxation by the maximum pressure shows that the curves of the different spacers overlap (Fig. 6b). Hence no significant differences in nesting are expected to take place, while some degree of nesting is expected compared to the plain fabric.

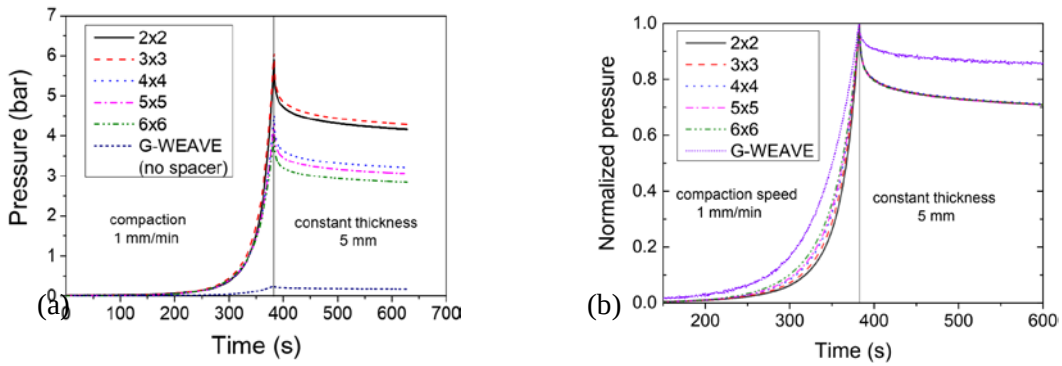

Figure 6. Curves of compaction (a) and relative relaxation (b) of sandwich preforms with spacers of varying mesh size and G-WEAVE plain fabric.

3.2 Flow experiments

Flow experiments showed that the core spacer visibly enhanced flow in the in-plane direction. The fluid always flowed from inlet to outlet in few seconds, leaving the fabric behind largely unsaturated. The spacer was responsible for an exaggerated duality in flow scales in the spacer's channels and through the fabric, where a combination of in-plane and out-of-plane flow was actually observed. In the first series of experiments, where no brake mechanism was adopted, the fluid continued to flow preferentially through the spacer rather than to impregnate the fabric layers. A large amount of fluid flowed out of the mold before the fabric was fully impregnated. As a result, there was no improvement in impregnation time, which was actually longer than for the plain fabric.

Saturated permeability for the five sandwich structures, measured from fluid flow rate at the outlet is reported in Fig. 7. The presence of spacers is responsible for an increase of more than one order of magnitude in saturated permeability compared to the plain fabric. The theoretical values were calculated from Darcy's law (Eq. 1) combined to the definition of hydraulic resistance for a rectangular channel, and neglecting the contribution of micro-flow [8]:

$$K_{channel} = \frac{(1 - 0.63\,{}^{h}/_{w})h^3 w}{12\,A} \tag{2}$$

where h and w are height and width of a channel and A is the area of a cross-sectional unit-cell of the sandwich (Fig. 2a and 4). Permeability values calculated from Eq. 2 are also reported in Fig. 7; they are in the same order of magnitude as the experimental values. However, theoretical permeability increases monotonically with channel width, whereas experimental values experienced a maximum for the spacer of mesh size 4 × 4. This could be caused by partial nesting of the tows in the spacers' pores, even though this was not observed in compaction experiments. Interestingly, there is a correspondence between the mesh size of maximum permeability and the tow width of the G-WEAVE (4 mm).

The results of the second series of flow experiments are summarized in Fig. 8. Without spacer, a standard slug-flow infiltration with narrow unsaturated region was observed (Fig. 8a), and full impregnation was achieved after around 60 s. When a spacer was added in the preform, after 3 s, the fluid had already reached the outlet and thanks to the brake mechanism (dam-zone in Fig. 8b and closed outlet in Fig. 8c) fabric impregnation could rapidly start to take place through combination of in-plane and out-of-plane flow. When a dam-zone was used as brake mechanism (Fig. 8b), after 15 s a dry spot was present, and it was still there after 60 s. Although the low permeability zone slowed down the fluid, it was not capable to completely block it. Therefore, the fluid was not forced to impregnate the highly-packed fabric. When in-plane flow was stopped by closing the outlet (Fig. 8c), full impregnation was achieved after just 15 s, and no major improvement was obtained after 60 s.

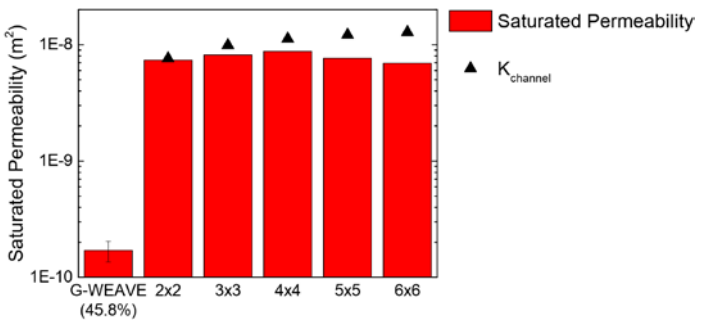

Figure 7. Saturated permeability of sandwich preforms as a function of mesh-size.

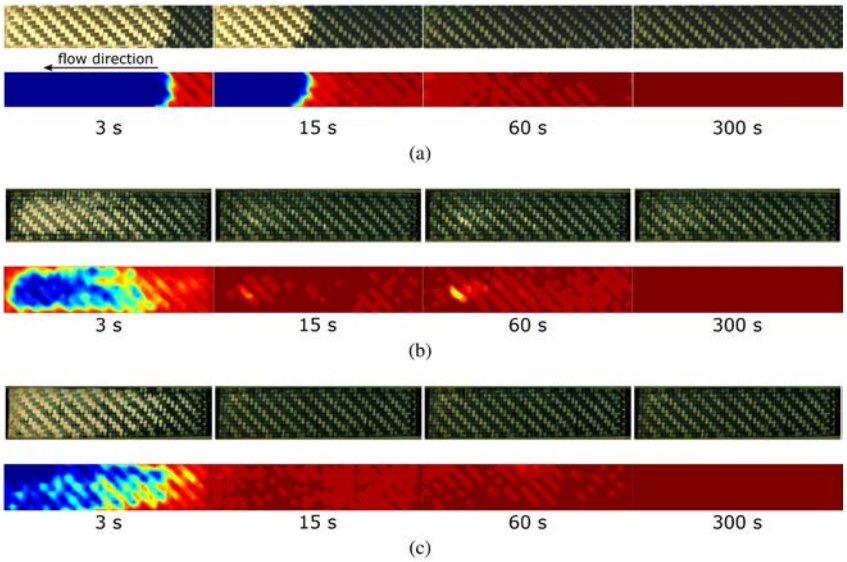

Figure 8. Visualization of the flow at different stages for experiments without any spacer (a) and with spacer and brake mechanism based on (b) dam-zone and (c) closed outlet (dark red = fully saturated, dark blue = dry).

3.3 Production of a plate

The flow pattern observed during impregnation of the sandwich preform with epoxy resin and using the "closed-outlet" strategy was similar to what was observed in the flow experiment with a model fluid (Fig. 8c). Macro-photos of the cross-section of the plate (Fig. 9a and b) show the shape of the channels formed by the PLA-spacer. Transverse and longitudinal fiber bundles partially nest in the channels, which, however, are not significantly blocked.

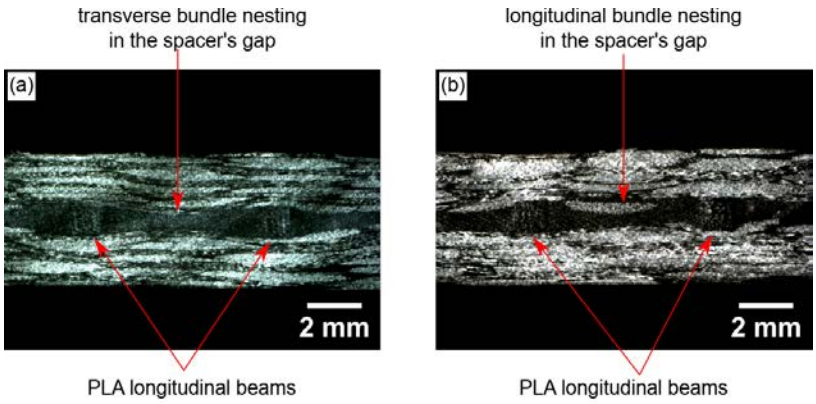

Figure 9. Macro-photos of the cross section of G-WEAVE with PLA-spacer after impregnation with epoxy resin, showing partial nesting of (a) transverse and (b) longitudinal bundles.

5. Conclusion

In this study, a preforming strategy involving the use of a second solid phase (spacer) as core of a sandwich stack was explored. Different architectures were compared in terms of compressive strength, compaction and permeability. Specifically, mesh size, and thus transverse gaps' size, was varied. This resulted in a varying number of longitudinal beams, which carry the load during compression, per unit area. Compaction tests on the sandwich preforms (spacer and fabric) provided a measure of the required

pressure to compact them in a mold; lower mesh size means larger number of beams per unit area, which is reflected in a higher compressive stiffness. Relaxation curves did not show any large difference between different mesh sizes. An increase of saturated permeability of more than one order of magnitude compared to the plain fabric was found for all the spacers. Apparently, the highest permeability was obtained in the case of the 4 × 4 spacer, but differences might as well fall within the experimental uncertainty, which reportedly can be as high as 20-30% [9]. Such a large increase of permeability relates to the presence of wide channels, where flow is predominant [8], and is accompanied by extreme dual-scale flow and difficulty in achieving full fabric impregnation with standard RTM injection. Two different impregnation strategies were therefore explored on the spacer 6 × 6 and compared to standard injection without any spacer. Flow visualization indicated that the fastest impregnation was obtained when vacuum was pulled from the outlet prior to and during the injection, thus reducing the risk of air entrapment; afterwards, the outlet was closed, so as to prevent outflow of fluid, and more fluid was injected from the inlet, thus forcing it to impregnate the fabric in out-of-plane direction. A reduction of the impregnation time of a factor 4 was achieved with a 6 × 6 PLA-spacer. A plate was produced via RTM with epoxy resin, demonstrating the feasibility of this concept.

Acknowledgements

This work is funded by the Swiss Competence Center for Energy Research (SCCER-Mobility) of the Swiss Innovation Agency (Innosuisse) and by Solvay (Research Center of Lyon, France). Chomarat is also thankfully acknowledged for having provided the glass-fabric.

References

[1] V. Michaud. Permeability properties of reinforcements in composites. In *Composite Reinforcements for Optimum Performance*, pp. 431-457. Woodhead Publishing, 2011.
[2] B.R. Gebart. Permeability of unidirectional reinforcements for RTM. *Journal of Composite Materials*, 26(8):1100–1133, 1992.
[3] J. Summerscales. A model for the effect of fibre clustering on the flow rate in resin transfer moulding. *Composites Manufacturing*, 4(1):27–31, 1993.
[4] P.R. Griffin, S.M. Grove, F.J. Guild, P. Russel, and J. Summerscales. The effect of microstructure on flow promotion in resin transfer moulding reinforcement fabrics. *Journal of Microscopy*, 177(3):207–217, 1995.
[5] E. Syerko, C. Binetruy, S. Comas-Cardona, and A. Leygue. A numerical approach to design dual-scale porosity composite reinforcements with enhanced permeability. *Materials and Design*, 131:307–322, 2017.
[6] D.M. Basford, P.R. Griffin, S.M. Grove, and J. Summerscales. Relationship between mechanical performance and microstructure in composites fabricated with flow-enhancing fabrics. *Composites*, 26(9):675–679, 1995.
[7] N. Patel and L. James Lee. Effects of fiber mat architecture on void formation and removal in liquid composite molding. *Polymer Composites*, 16(5):386–399, 1995.
[8] D. Salvatori, B. Caglar, H. Teixidó, and V. Michaud. Permeability and capillary effects in a channel-wise non-crimp fabric. *Composites Part A: Applied Science and Manufacturing*, 108:41–52, 2018.
[9] R. Arbter et al. Experimental determination of the permeability of textiles: A benchmark exercise. *Composites Part A: Applied Science and Manufacturing*, 42(9):1157–1168, 2011.